J|A|C|S ARTICLES

Published on Web 11/23/2009

Formation of Well-Oriented Microtubules with Preferential Polarity in a Confined Space under a Temperature Gradient

Akira Kakugo,[†,‡] Yoshiki Tamura,[†] Kazuhiro Shikinaka,[†,§] Momoko Yoshida,[†] Ryuzo Kawamura,[†,||] Hidemitsu Furukawa,[†] Yoshihito Osada,[†,||] and Jian Ping Gong*[,†]

Department of Biological Science, Graduate School of Science, Hokkaido University, and PRESTO, Japan Science and Technology Agency, Sapporo 060-0810, Japan

Received February 27, 2009; E-mail: gong@sci.hokudai.ac.jp

Abstract: Tubulin polymerization in a confined space under a temperature gradient produced well-oriented microtubule assemblies with preferential polarity. We analyzed the structure and polarity of these assemblies at various levels of resolution by performing polarized light microscopy (millimeter order), fluorescence microscopy (micrometer order), and transmission electron microscopy (nanometer order).

Introduction

In living systems, emergent functions can be attributed to the well-organized complex structure of the organisms.[1] For example, in muscle tissue, actin−myosin interactions trigger molecular changes that lead to macroscopic deformations; these deformations occur in a hierarchical pattern in which the actin and myosin molecules are organized with a highly regulated spatial distribution and definite polarity.[2−4] The integration of these deformations is responsible for the dynamic motion of the muscle tissue.

A microtubule (MT) is a stiff, hollow, cylindrical protein filament with a diameter of 25 nm; such a filament is formed by the self-assembly of heterodimers of nanosized globular proteins called tubulins. In living cells, the assembly of rodlike biomolecules such as MTs and F-actins from their respective monomeric units is spatially and temporally regulated by the localization of binding proteins and the coupling of the binding proteins to their signaling molecules, respectively.[5−7] These rodlike biomolecules show intrinsic polarity, which can be attributed to the extremely specific cellular localization of the binding proteins and signaling molecules during the process of nucleation and anisotropic elongation.[8] In this process, the first step is the formation of the nucleus (oligomers); overcoming the free-energy barrier for this step takes time. Usually, an increase in the concentration of monomers increases the frequency of collisions between them and facilitates nucleus formation. After the formation of the nucleus, the thermodynamically favorable elongation (growth) process proceeds rapidly. In a concentration gradient, nucleation occurs in the region with a high concentration of monomers, and the growth progresses toward the low-concentration region. In in vitro systems with tubulin concentrations above a certain threshold level, nucleation and polymerization can be initiated by increasing the temperature or the ionic strength in the presence of guanosine-5-triphosphate (GTP). After nucleation, the two ends of the MTs grow at different rates: the end that shows rapid growth is called the plus end, and the end that shows slow growth is called the minus end.[9] Kinesin, an MT-based motor protein, moves toward the plus end. This growth pattern leads to the formation of a rodlike structure. The anisotropic growth and rodlike structure facilitate the construction of a large, highly ordered MT assembly that shows well-defined polarity under asymmetric polymerization conditions.

In a recent study, we used a low actin concentration and showed that F-actins form a network under unidirectional diffusion of F-actin cross-linkers (polycations), which behave like binding proteins; however, homogeneous mixing with polycations yielded only bundles of F-actins.[10] Therefore, an asymmetric spatial distribution of polycations is important for generating architectural variety in F-actin assemblies.

In this study, we employed asymmetric polymerization conditions and spatial restriction to mimic the natural system for constructing a well-oriented three-dimensional MT assembly

† Hokkaido University.
‡ PRESTO, Japan Science and Technology Agency.
§ Present address: Institute of Symbiotic Science and Technology, Tokyo University of Agriculture and Technology, Koganei 184-8588, Japan.
|| Present address: RIKEN, Saitama 351-0198, Japan.

(1) Walleczek, J. *Self-Organized Biological Dynamics and Nonlinear Control: Toward Understanding Complexity, Chaos and Emergent Function in Living Systems*, 1st ed.; Cambridge University Press: Cambridge, U.K., 2006.
(2) Huxley, H. E. *Science* **1969**, *164*, 1356–1366.
(3) Huxley, A. F. *Reflections on Muscle*; Liverpool University Press: Liverpool, U.K., 1980.
(4) Pollack, G. H. *Cells, Gels and the Engines of Life*; Ebner and Sons Publishers: Seattle, WA, 2001.
(5) Chung, C. Y.; Funamoto, S.; Firtel, R. *Trends Biochem. Sci.* **2001**, *26*, 557–566.
(6) Kurokawa, K.; Nakamura, T.; Aoki, K.; Matsuda, M. *Biochem. Soc. Trans.* **2005**, *33*, 631–634.
(7) Svitkina, T.; Borisy, G. *J. Cell Biol.* **1999**, *145*, 1009–1026.
(8) Kwon, H. J.; Tanaka, Y.; Kakugo, A.; Shikinaka, K.; Furukawa, H.; Osada, Y.; Gong, J. P. *Biochemistry* **2006**, *45*, 10313–10318.
(9) Lodish, H.; Berk, A.; Kaiser, C. A.; Krieger, M.; Scott, M. P.; Bretscher, A.; Ploegh, H.; Matsudaira, P. T. *Molecular Cell Biology*, 4th ed.; W. H. Freeman: San Francisco, 1999.
(10) Kwon, H. J.; Kakugo, A.; Ura, T.; Okajima, T.; Tanaka, Y.; Furukawa, H.; Osada, Y.; Gong, J. P. *Langmuir* **2007**, *23*, 6257–6262.

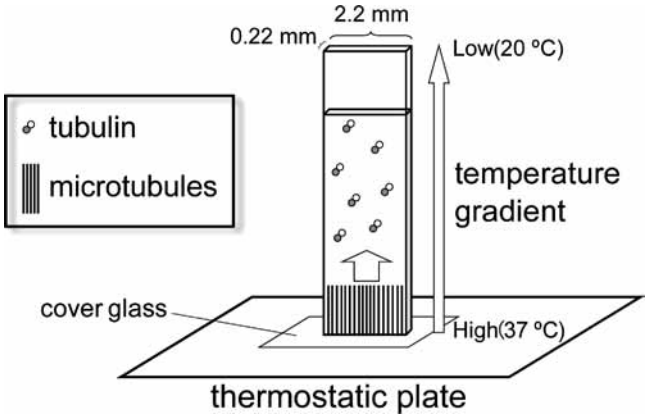

Figure 1. Schematic illustration of the experimental setup for preparing well-oriented MTs under asymmetric polymerization conditions (a temperature gradient) in a confined space.

with preferential polarity. To this end, we polymerized MTs in a cubic cell under a temperature gradient. Under this gradient, the nucleus was formed at the warm end, and the growth process progressed toward the cold end. The hierarchically ordered structure of the MT assembly was characterized by polarized light microscopy (PLM; millimeter order), fluorescence microscopy (FM; micrometer order), and transmission electron microscopy (TEM; nanometer order). The polarity of the MT assembly was assessed by monitoring the sliding motion of green fluorescent protein-labeled kinesins (GFP-kinesins) along the MTs.

Results and Discussion

Formation of the Anisotropic Structure. To create asymmetric polymerization conditions, we used a 25 mm long glass cell with inner cross-sectional dimensions of 2.2 mm × 0.22 mm; the inner width of the cell was less than the persistence length of the MT (~5 mm). The cell was placed on ice, and a tubulin solution (380 μM) in a polymerizing buffer containing GTP (1 mM) was introduced into the cell. Next, the cell was vertically placed on a thermostatic plate set at 37 °C, and tubulin nucleation and polymerization were initiated from the warm end of the cell. The tubulin concentration used in this study was much higher than that required for treadmilling of MT.[11] Polymerization of the tubulins was performed in the presence of microtubule-associated-protein (MAP) to avoid dynamic catastrophe of formed MTs (see Materials and Methods in the Supporting Information).[12] Under these conditions, localized tubulin nucleation was initiated at the warm end of the cell. The experimental system is illustrated in Figure 1. When the density or length of the rigid rod exceeds a critical value, the rods spontaneously align parallel to one another and form a liquid-crystalline phase.[13] This phenomenon can be attributed to the excluded-volume (entropic) effect on the molecules.

To detect the transition from the isotropic phase to the liquid-crystalline phase (oriented ordering), we monitored the birefringence changes in the tubulin solution using PLM. Figure 2a shows that polymerization occurred in a thermostatic room at 37 °C for 15 min. A weak anisotropic birefringence and small brightly colored domains (500−1000 μm^2) are randomly distributed in the cell. Thus, in the absence of a temperature gradient, the MTs are oriented in a particular direction within the domains, but the domains themselves lie in all possible directions.

Figure 2b shows the PLM image of the MTs formed under the temperature gradient. The brightly colored region at the bottom of the cell (warm end) extended gradually and continuously toward the top (cold end) of the cell. This sample showed strong anisotropic birefringence and distinct alternating dark and bright bands under a cross-polarizing microscope. Complete extinction was observed at 0° and 90°, while maximum brightness was observed at 45°; this finding indicated that the MTs were oriented either parallel or perpendicular to the direction of the polarizer.

Figure 2c illustrates the progression of the birefringence region from the warm end to the cold end of the cell (also see Movie 1 in the Supporting Information). The intensity and growth rate of the birefringence region decreased with the temperature (for details, see Figure 5).

Since thermal convection due to the temperature gradient may influence the alignment of MTs, we studied the effect of thermal convection on the anisotropic alignment of MTs. To this end, we warmed the upper end of the cell to the optimum temperature (37 °C) while maintaining the lower end at the environmental temperature (21 °C); thermal convection was not expected to occur under these conditions. A birefringence region began to develop from the upper (warm) end of the cell, and an anisotropic structure was formed. This observation indicated that thermal convection did not influence these findings. Over a prolonged observation period (>2 h), the continuous birefringence pattern transformed into a horizontally striped pattern (data not shown). Similar patterns have been reported previously and have been attributed to the putative formation of nonequilibrium energy-dissipating structures through GTP hydrolysis.[14]

The cell dimensions also played an important role in MT alignment. Even in the absence of the temperature gradient, MTs preferentially aligned themselves along the longitudinal axis of the cell; this phenomenon was attributed to the fact that the MTs were within a confined space. However, this preferential orientation was more obvious in the presence of a temperature gradient. In contrast, when a cell with a width of >7 mm was used for tubulin polymerization, isotropic birefringence was observed even under asymmetric polymerization conditions. This finding indicates that MT alignment can occur only within a specific range of cell dimensions.

Structural Analysis. The MT assembly was removed from the cell and observed using FM. To visualize the MT assembly, we performed polymerization using rhodamine-labeled tubulin. Figure 3 clearly shows that the MTs were aligned along the longitudinal axis. The detailed structure of the MT assembly was confirmed on a subnanometer scale using TEM (Figure S1 in the Supporting Information). These results were consistent with those of FM and PLM, thereby confirming the anisotropic alignment of the MTs.

As mentioned previously, the regular and parallel head-to-tail orientations of the tubulin molecules confer distinct structural polarity to MTs; this polarity is responsible for the unidirectional motion of MT-based motor proteins such as kinesin and dynein. Thus, to ensure efficient motor-protein coupling, the polarity of MTs should be regulated.

(11) Hotani, H.; Horio, T. *Cell Motil. Cytoskeleton* **1988**, *10*, 229–236.
(12) Horio, T.; Hotani, H. *Nature* **1986**, *321*, 605–607.
(13) Onsager, L. *Ann. N.Y. Acad. Sci.* **1949**, *51*, 627–659.
(14) Tabony, J.; Job, D. *Proc. Natl. Acad. Sci. U.S.A.* **1992**, *89*, 6948–6952.

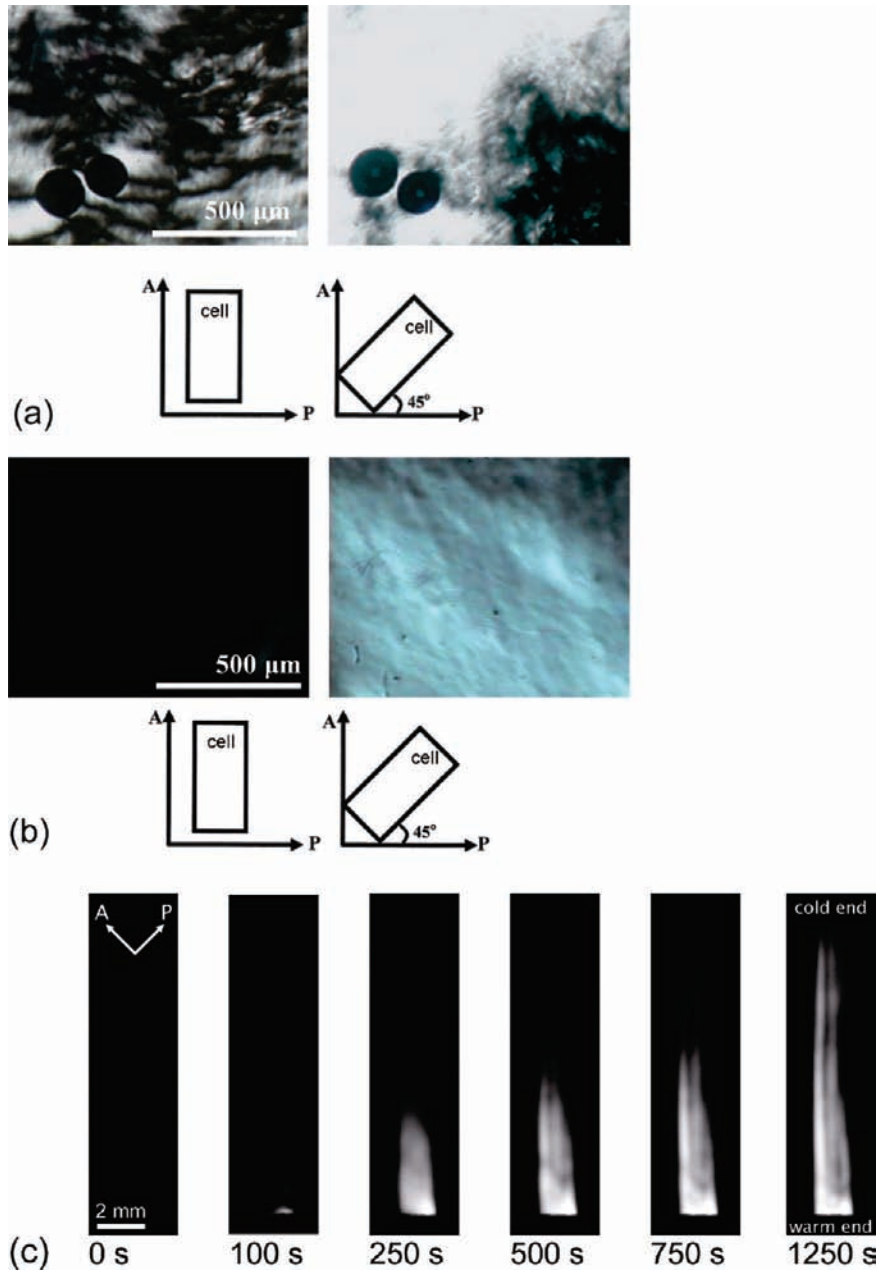

Figure 2. Cross-polarizing microscopic images of the MT assembly. (a) MT assembly prepared without a temperature gradient in a confined space: (left) cell placed parallel to the analyzer; (right) cell placed diagonal to the analyzer. (b) MT assembly prepared using a temperature gradient in a confined space: (left) temperature gradient parallel to the analyzer; (right) temperature gradient diagonal to the analyzer. (c) Time-lapse images of the growth of the MT assembly prepared using a temperature gradient in a confined space. The cell was diagonal to the analyzer.

To elucidate the preferential polarity of the MT assembly, we used FM to monitor the sliding motion of GFP-kinesins along the MT tracks (Figure 4 and Movies 2−4 in Supporting Information). In this study, measurements were obtained from the middle region of the rectangular cell (~12 mm from the warm end), where the MTs were to be polymerized with preferential polarity. To increase the signal-to-noise ratio for GFP detection, MT assemblies with low filament density were two-dimensionally fixed on the glass surface of the cell using *n*-ethylmaleimide (NEM)-kinesins (for details, see Materials and Methods in the Supporting Information). The density of these MTs was controlled by regulating the concentration of the NEM-kinesins. As shown in Figure 4b and Movie 3, in the presence of ATP, most of the GFP-kinesins moving along the MT tracks moved toward the cold end of the cell (the upward direction in the figures and movies). Among the 287 MT tracks identified using the FM images of GFP-kinesin, 259 were oriented toward the cold end and 28 were oriented toward the warm end (the ratio of tracks oriented toward the cold end to those oriented toward the warm end was 90:10). As expected, the plus ends of the MT assemblies were preferentially directed toward the cold end (i.e., in the direction of the thermal gradient). The mean velocity of the GFP-kinesins moving along the MT assembly was 0.37 ± 0.17 μm s^{-1} ($n = 30$).

Thus, we have successfully shown that the application of asymmetric polymerization conditions within a confined space can yield a well-oriented MT assembly with preferential polarity.

Figure 3. FM images of the MT assembly prepared using a temperature gradient in a confined space.

Factors Influencing the Preferential Polarity. As described previously, after an MT nucleus is formed, the two ends of the MT grow at different rates.[15,16] The rate of MT elongation (in terms of subunits per second) was evaluated using the equation $v(t) = k_{on}[T] - k_{off}$, where k_{on} and k_{off} are the association and dissociation rate constants at 37 °C, respectively, and [T] is the concentration of free tubulin. The k_{on} and k_{off} values at the plus end of the microtubules were 8.9 μM^{-1} s^{-1} and 44 s^{-1}, respectively, and the values at the minus end were 4.3 μM^{-1} s^{-1} and 23 s^{-1}, respectively.[16] The rate of elongation (μm s^{-1}) was obtained by dividing the rate constants by an empirical factor (i.e., 1634 tubulins/μm of the MT). At a tubulin concentration of 380 μM, the elongation rates at the plus end (v_{plus}) and the minus end (37 °C) were 2.0 and 0.98 μm s^{-1}, respectively. In a tubulin concentration gradient, the polymerization rate increases with the concentration; therefore, growth preferentially occurs toward the higher concentration. Since the plus end grows faster than the minus end, the growth at the minus end is suppressed by the tubulin consumption at the plus end. Therefore, the MT structure may show preferential growth of the plus end; in a temperature gradient, this preferential growth would occur toward the cold end. The degree of polarity depends on the ratio of the number of nuclei to the number of free tubulin units.

(15) Mitchison, T.; Kirschner, M. *Nature* **1984**, *312*, 237–242.
(16) Walker, R. A.; O'Brien, E. T.; Pryer, N. K.; Soboeiro, M. F.; Voter, W. A.; Erickson, H. P.; Salmon, E. D. *J. Cell Biol.* **1988**, *107*, 1437–1448.

The formation of an MT array with preferential polarity is based on the premise that the propagation of heat for the nucleation toward the cold end is slower than the polymerization rate of the MT. When the former value exceeds the latter, nucleation is faster than MT growth, thereby leading to random polarity. To study this aspect, we measured the temperature propagation in the glass cell by using a thermotracer (Figure 5a) and determined the MT elongation rate toward the cold end (Figure 5b). The elongation was evaluated by monitoring the growth of the birefringence region ($B_{1/2}$), as described in Materials and Methods in the Supporting Information. As shown in Figure 5b, within the first 100 s, the boundary of the region at 37 °C (T_{37}) rapidly progressed at a rate of ~50 μm s^{-1} ($v_{T_{37}}^{initial}$) and covered a distance of ~2 mm from the warm end. After 100 s, T_{37} progressed very little, and the propagation rate ($v_{T_{37}}$) was less than 0.3 μm s^{-1}.

As shown in Figure 5b, $B_{1/2}$ growth lagged behind T_{37} propagation by ~180 s; however, the $B_{1/2}$ growth rate was subsequently accelerated to ~44 μm s^{-1} ($v_{B_{1/2}}^{initial}$) until a distance of ~4 mm from the warm end was reached. Thereafter, $B_{1/2}$ showed almost constant growth at a rate of 2.0 μm s^{-1} ($v_{B_{1/2}}$). Since the growth rate at the initial stage (44 μm s^{-1}) was much higher than the polymerization rate of MT (v_{plus}) (~2 μms^{-1}),[14] we think that the nucleation process was dominant at this stage. In contrast, the growth rate in the later stages was linear ($v_{B_{1/2}} \approx 2$ μm s^{-1}) and approximately equal to the rate of MT polymerization from the plus end ($v_{plus} \approx v_{B_{1/2}}$). Thus, $B_{1/2}$ propagation during the later stages depended on polymerization from the existing nuclei. The difference between the distances at which the T_{37} propagation was initiated and the $B_{1/2}$ propagation began to decelerate (2 and 4 mm, respectively) indicates that nucleation may occur at a temperature lower than 37 °C. Therefore, at distances greater than 4 mm, when the growth process begins to slow, the MT may show preferential polarization; this assumption is in agreement with the results shown in Figure 4. An MT array with random polarity [cold end/warm end = 48% (n = 62):52% (n = 66)] was also observed in the bottom region of the rectangular cell (~3 mm from the warm end).

On the basis of the above discussion, we have presented a schematic illustration of MT growth in Figure 5c. Initially, when T_{37} propagation is much faster than the MT polymerization rate, the nucleation kinetics is the rate-determining factor for the growth process. Thus, $B_{1/2}$ propagation depends on the propagation of nuclei. Under these conditions, MTs start to elongate from thermally induced nuclei and align themselves parallel to the long axis of the glass cell with random polarity. The random polarity is observed because (1) there is no directional tubulin concentration gradient around the nuclei and (2) microtubule elongation can occur in both directions. In the later stages, when the T_{37} propagation is slower than the MT polymerization rate, no new nuclei are formed at the growth front, and MT growth depends exclusively on polymerization. At this stage, a tubulin concentration gradient develops at the growth front. Since MTs grow 2 times faster at the plus end than at the minus end, the plus end grows preferentially, and the growth of the minus end is suppressed in the absence of excess free tubulin. Consequently, MTs are formed with their plus ends oriented toward the cold end of the glass cell.

Finally, we discuss how the temperature gradient facilitates the orientation. The mechanism of MT orientation can be explained by the strong interaction between MTs and the cell wall (wall effect). This interaction sterically hinders the

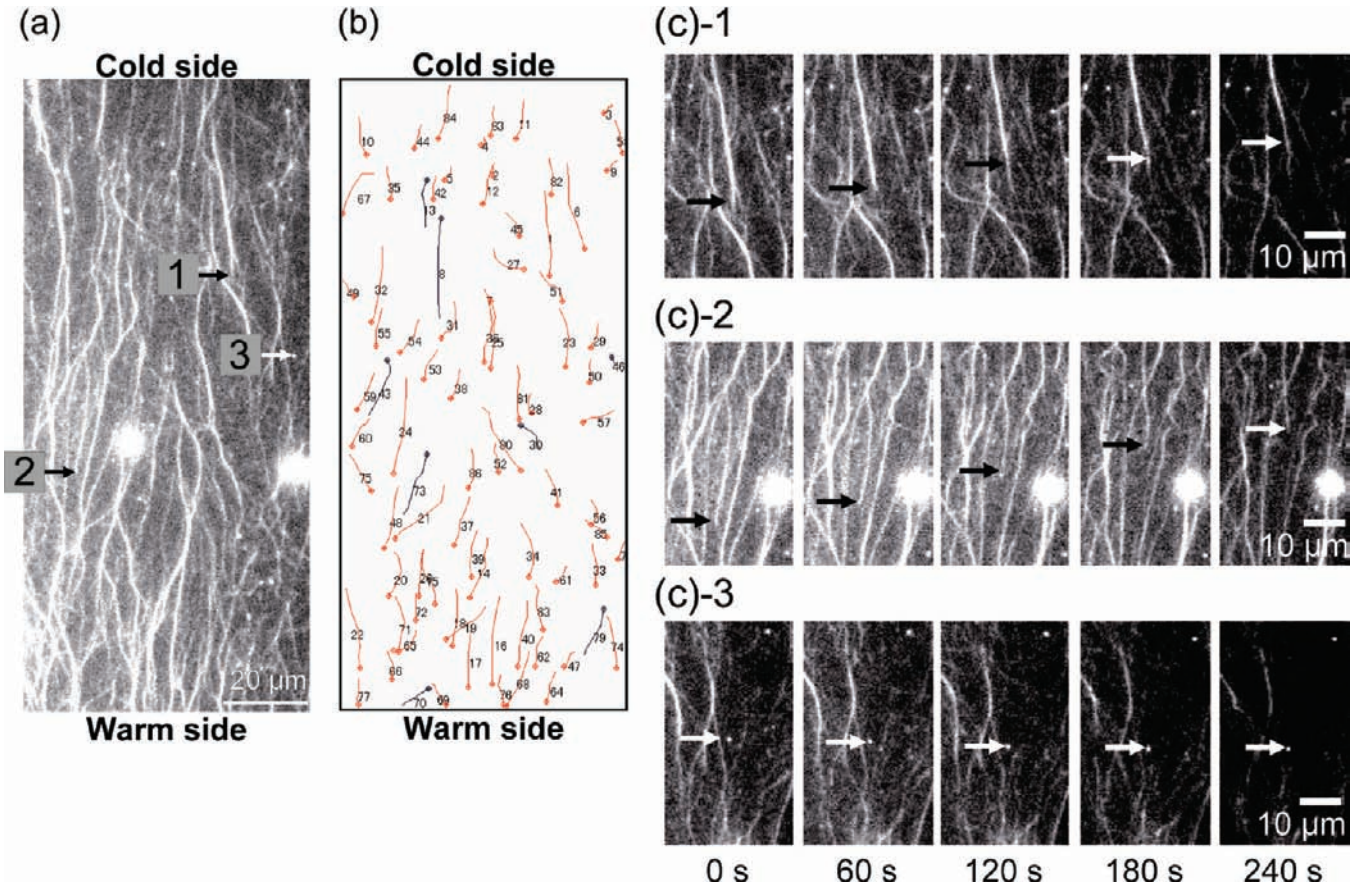

Figure 4. Motility of GFP-kinesins on the MT assembly. (a) FM image of GFP-kinesins on MTs. (b) FM images of the trajectories of the sliding motion of the GFP-kinesins along the MT tracks on the assembly. These trajectories were obtained by superimposing sequential images of the GFP-kinesins shown in (a). The red trajectories indicate sliding motion toward the cold end of the glass cell, and the blue trajectories indicate the sliding motion toward the warm end of the glass cell. In this figure, among the 94 MT tracks, 86 tracks were oriented toward the cold end and 8 toward the warm end. (c) Time-sequence images of sliding motion at 60-s intervals: [(c)-1, (c)-2] enlarged fluorescence images of GFP-kinesins moving toward the cold end; [(c)-3] GFP-kinesins moving toward the warm end along the MT tracks. The numbering used in (c) corresponds to the numbering used with the pointing arrows in (a). Observations were recorded at the middle region of the rectangular cell (∼12 mm from the warm end).

rotational diffusion of the rodlike MTs along the glass wall. Consequently, MTs align themselves parallel to the wall over an extended distance. Subsequently, because of kinetic preferences, MTs favorably grow toward the region with high tubulin concentration. At the polymerization-dominant stage, the nuclei are localized at the lower region of the cell, and polymerization occurs toward the upper region; therefore, the tubulin concentration in the upper region is higher than that in the lower region. Consequently, MTs predominantly elongate along the axis of the glass cell toward the colder end. Thus, a temperature gradient also favors preferential orientation.

Motor proteins, including the MT-kinesin system, have been proposed as the building blocks of ATP-fueled moving systems.[17−20] Some studies have attempted to increase the size, dimension, and complexity of the motor-protein-based moving systems.[19,21] Recently, several methods involving passive[22] and active[23−25] self-assembly processes have been developed to fabricate motor-protein assemblies with well-controlled polarity; these assemblies also show preferential motion. However, since motor-protein interactions are primarily two-dimensional, these studies have not investigated many motor proteins. In the present study, under asymmetric polymerization conditions, MTs organized themselves into large three-dimensional structures with well-ordered polarity; furthermore, this self-organization was achieved without the assistance of any compulsive microfabrication techniques such as lithography.[26−29]

We expect that the present work will widen the range of potential applications of motor proteins in biodevices or biomachines (for analyzing or powering systems that are partly synthetic and partly biological).

(17) Yano, M.; Yamamoto, Y.; Shimizu, H. *Nature* **1982**, *299*, 557–559.
(18) Suzuki, H.; Yamada, A.; Oiwa, K.; Nakayama, H.; Mashiko, S. *Biophys. J.* **1997**, *72*, 1997–2001.
(19) Brown, T. B.; Hancock, W. O. *Nano Lett.* **2002**, *2*, 1131–1135.
(20) Diehl, M. R.; Zhang, K.; Lee, H. J.; Tirrell, D. A. *Science* **2006**, *311*, 1468–1471.
(21) Roos, W.; Roth, A.; Sackmann, E.; Spatz, J. P. *ChemPhysChem* **2003**, *4*, 872–877.
(22) Kakugo, A.; Sugimoto, S.; Gong, J. P.; Osada, Y. *Adv. Mater.* **2002**, *14*, 1124–1126.
(23) Hess, H.; Clemmens, J.; Brunner, C.; Doot, R.; Luna, S.; Ernst, K. H.; Vogel, V. *Nano Lett.* **2005**, *5*, 629–633.
(24) Kawamura, R.; Kakugo, K.; Shikinaka, K.; Osada, Y.; Gong, J. P. *Biomacromolecules* **2008**, *9*, 2277–2282.
(25) Kawamura, R.; Kakugo, K.; Osada, Y.; Gong, J. P. *Langmuir* [Online early access]. DOI: 10.1021/la902179f. Published Online: Oct 8, 2009.
(26) Turner, D. C.; Chang, C.; Fang, K.; Brandow, S. L.; Murphy, D. B. *Biophys. J.* **1995**, *69*, 2782–2789.
(27) Stracke, R.; Böhm, K. J.; Burgold, J.; Schacht, H.-J.; Unger, E. *Nanotechnology* **2000**, *11*, 52–56.
(28) Limberis, L.; Magda, J. J.; Stewart, R. J. *Nano Lett.* **2001**, *1*, 277–280.
(29) Yokokawa, R.; Takeuchi, S.; Kon, T.; Nishiura, M.; Sutoh, K.; Fujita, H. *Nano Lett.* **2004**, *4*, 2265–2270.

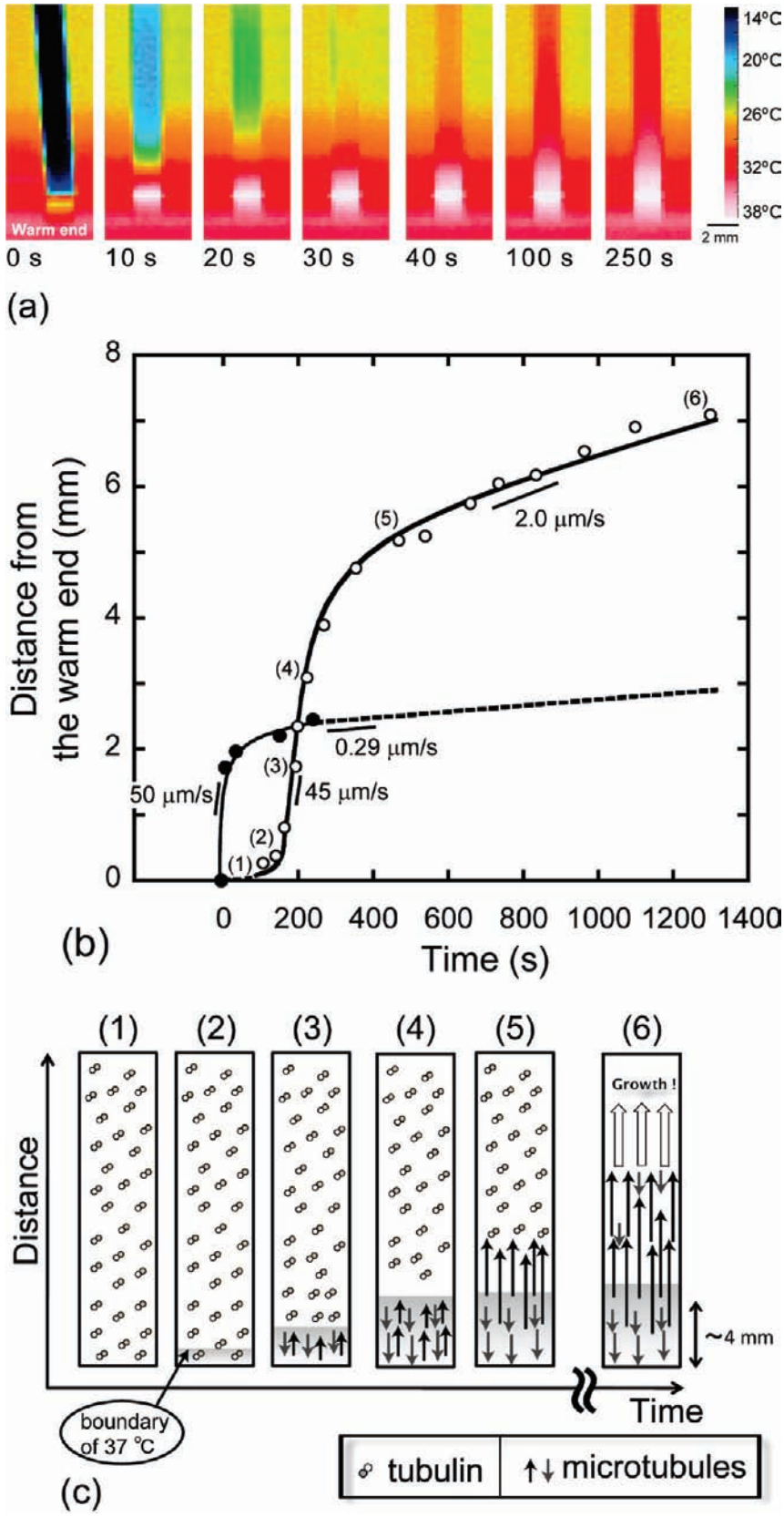

Figure 5. (a) Time-lapse images of thermal propagation and the temperature gradient in the glass cell, which was monitored by a thermotracer. (b) Time courses of the propagation of the 37 °C boundary (T_{37}) (closed circles) and the growth of the birefringence region ($B_{1/2}$) (open circles) in the glass cell. The birefringence region was evaluated by monitoring the progression of the boundary showing half of the maximum brightness in the PLM image. The dashed curves have been drawn for guidance. (c) Schematic representation of the possible growth process and the orientation of MTs in the assembly. The numbering used for the growth stages in (c) corresponds to the numbers adjacent to the plot in (b). In the initial stage [(2), (3), (4)], $v_{T_{37}}^{\text{initial}} \gg v_{\text{plus}}$, i.e., the nucleation process is dominant. In the later stage [(5), (6)], $v_{T_{37}} \ll v_{\text{plus}}$, i.e., the polymerization process is dominant. The MTs formed at the later stage show preferential polarity.

Acknowledgment. We appreciate the valuable suggestions of K. Takiguchi, Y. Takiguchi, and Y. Mimori-Kiyosue. This research was financially supported by PRESTO, JST, and the Ministry of Education, Science, Sports and Culture, Japan (Grant-in-Aid for Specially Promoted Scientific Research, 18002002).

Supporting Information Available: Materials and Methods, cross-sectional TEM images of the MT assembly, movies showing the growth of the MT assembly (AVI), motility assay of GFP-kinesins, and trajectories of the sliding motion of the GFP-kinesins. This material is available free of charge via the Internet at http://pubs.acs.org.

JA901538N